

Electronic Supplementary Information:

Seleno twisted benzodiperyleneimides: a facile synthesis and excellent electron acceptors for additive-free organic solar cells

Ming Hu^{a,†}, Xiaohong Zhao^{a,†}, Guomin Zhu^a, Youdi Zhang^{a,b}, Zhongyi Yuan^{*a,b}, Lei Wang^a, Xiaoshuai Huang^a, Yu Hu^a, and Yiwang Chen^{*a,b}

^aCollege of Chemistry, Nanchang University, 999 Xuefu Avenue, Nanchang 330031, China

^bInstitute of Polymers and Energy Chemistry (IPEC), Nanchang University, 999 Xuefu Avenue, Nanchang 330031, China

*Corresponding author.

E-mail: yuan@ncu.edu.cn (Z. Yuan)

Tel.: +86 791 83968703; Fax: +86 791 83969561.

E-mail: ywchen@ncu.edu.cn (Y. Chen)

[†]Author contributions. M. Hu and X. Zhao contributed equally to this work.

Content

Experimental Details.....	3
S1. Materials and methods	3
S2. Synthetic Procedures.....	3
S3. NMR spectra	5
S3.1. ¹ H NMR of 3 in CDCl ₃ (400 MHz).....	5
S3.2. ¹³ C NMR of 3 in CDCl ₃ (100 MHz)	5
S3.3. ¹ H NMR of 4 in CDCl ₃ (400 MHz).....	6
S3.4. ¹³ C NMR of 4 in CDCl ₃ (100 MHz)	6
S3.5. ¹ H NMR of 5 in CDCl ₃ (400 MHz).....	7
S3.6. ¹³ C NMR of 5 in CDCl ₃ (100 MHz)	7
S3.7. ¹ H NMR of 6 in CDCl ₃ (400 MHz).....	8
S3.8. ¹³ C NMR of 6 in CDCl ₃ (400 MHz)	8
S3.9. ¹ H NMR of TBDPDI-Se-C ₁₁ in CDCl ₃ (400 MHz)	9
S3.10. ¹³ C NMR of TBDPDI-Se-C ₁₁ in CDCl ₃ (100 MHz)	9
S3.11. ¹ H NMR of TBDPDI-Se-C ₂₃ in CDCl ₃ (400 MHz)	10
S3.12. ¹³ C NMR of TBDPDI-Se-C ₂₃ in CDCl ₃ (100 MHz)	10
S4. TGA curves of TBDPDI-Se-C ₁₁ and TBDPDI-Se-C ₂₃	11
S5. DSC curves of TBDPDI-Se-C ₁₁ and TBDPDI-Se-C ₂₃	11
S6. UV-visible absorption.	11
S7. DFT calculations	12
S8. Cyclic voltammetry.....	13
S9. Optimization of the fabricating conditions of solar cells	13
S10. <i>J-V</i> Curves for carrier mobility	15
S11. Charge separation and recombination dynamics.....	16
S12. AFM images of the blend films	17
S13. TEM images of the blend films.....	18
Reference	18

Experimental Details

S1. Materials and methods

Chlorobenzene, Ag (99.999%), MoO₃ (99.999%), indium-tin oxide (ITO) glass, and other materials were purchased from commercial suppliers. PBDB-T was synthesized with the reported method.¹

The ¹H and ¹³C NMR were measured on NMR Spectrometer with tetramethylsilane (TMS) as the internal standard. Mass spectra were recorded with a MALDI-TOF mass spectrometer in linear mode. UV-vis absorption was recorded on a Perkin Elmer Lambda 750 spectrophotometer. All the measurements were carried out at room temperature.

S2. Synthetic Procedures

Synthesis of 3. A mixture of **2** (4.02 g, 5.76 mmol), selenium power (4.55 g, 57.63 mmol), and 40 mL *N*-methyl pyrrolidone (NMP) was stirred at 170 °C for 8 h under argon. The mixture was extracted with CH₂Cl₂, washed with water, and purified through the silica gel column. The eluent was petroleum ether/CH₂Cl₂ (1:1, v/v). Compound **3** (3.24 g, 77%) was obtained as a yellow solid. ¹H NMR (400 MHz, CDCl₃) δ 8.44 (s, 2H), 8.36 (d, 2H), 8.14 (d, 2H), 4.43 (m, 8H), 1.86 (s, 8H), 1.55 (d, 8H), 1.04 ppm (d, 12H). ¹³C NMR (100 MHz, CDCl₃) δ 168.6, 137.4, 132.1, 129.2, 125.6, 121.4, 65.5, 30.7, 19.3, 13.8 ppm. HRMS (MALDI-TOF): Calcd for C₃₂H₄₉N₃O₂: 730.2045, found: 730.2059 (M⁺). MP: 225 °C.

Synthesis of 4. A mixture of **3** (3.01 g, 4.12 mmol), Br₂ (65.92g, 412.48 mmol), and 50 mL CH₂Cl₂ was stirred at 0 °C for 15 min. The mixture was extracted with CH₂Cl₂, washed with water, and purified through the silica gel column. The eluent is petroleum ether/CH₂Cl₂ (2:1, v/v). Compound **4** (2.47 g, 74%) was obtained as a yellow solid. ¹H NMR (400 MHz, CDCl₃) δ 9.91 (d, 1H), 8.61 (d, 2H), 8.53 (s, 1H), 8.25 (d, 1H), 4.43 (d, 8H), 1.87 (m, 8H), 1.55 (m, 8H), 1.03 ppm (m, 12H). ¹³C NMR (100 MHz, CDCl₃) δ 168.3, 167.2, 138.0, 137.2, 136.9, 130.3, 129.9, 128.5, 126.42, 125.1, 118.8, 65.7, 30.6, 19.3, 13.8 ppm. HRMS (MALDI-TOF): Calcd for C₃₂H₄₉N₃O₂: 808.1150, found: 808.1167 (M⁺). MP: 115 °C.

Synthesis of 5. A mixture of **4** (0.53 g, 0.65 mmol), 1,4-benzenediboronic acid bis(pinacol) ester (0.098 g, 0.30 mmol), Pd(PPh₃)₄ (0.028 g, 0.024 mmol), K₂CO₃ (0.49 g, 3.56 mmol), 4 mL THF, and 2 mL H₂O was stirred at 85 °C for 13 h under argon. The mixture was extracted with CH₂Cl₂, washed with water, and purified through the silica gel column. The eluent is CH₂Cl₂. Compound **5** (0.26 g, 75%) was obtained as a yellow solid. ¹H NMR (400 MHz, CDCl₃) δ 8.78 (d, 4H), 8.48 (s, 2H), 8.13 (s, 2H), 7.96 (s, 2H), 7.81 (s, 4H), 4.41 (d, 16H), 1.81 (d, 16H), 1.50 (m, 16H), 1.01 ppm (d, 24H). ¹³C NMR (100 MHz, CDCl₃) δ 168.58, 143.12, 138.72, 138.69, 137.82, 137.13, 133.89, 130.48, 129.06, 128.70, 127.94, 125.79, 125.30, 65.67, 30.56, 29.60, 19.30, 13.73 ppm. HRMS (MALDI-TOF): Calcd for C₃₂H₄₉N₃O₂:1534.4246, found: 1534.4260 (M⁺). MP: 150 °C.

Synthesis of 6. A mixture of **5** (0.20 g, 0.13 mmol), I₂ (0.01 g, 0.039 mmol), and 800 mL CH₂Cl₂ was exposed to sunlight for 8 h. The mixture was extracted with CH₂Cl₂, washed with water, and recrystallized from toluene and acetic acid. Compound **6** (0.16 g, 80%) was obtained as a yellow solid. ¹H NMR (400 MHz, CDCl₃) δ 10.06 (s, 2H), 9.70 (s, 2H), 9.49 (s, 3H), 9.31 (d, 2H), 4.62 (m, 12H), 4.03 (m, 4H), 1.95 (m, 7H), 1.25 (m, 24H), 1.03 (m, 11H), 0.84 ppm (m, 14H). ¹³C NMR (100 MHz, CDCl₃) δ 168.53, 167.94, 138.55, 133.61, 133.35, 129.61, 128.03, 127.21, 126.01, 125.32, 125.03, 123.39, 65.85, 30.52, 29.72, 19.39, 19.35, 18.65, 13.97, 12.95, 1.02 ppm. HRMS (MALDI-TOF): Calcd for C₃₂H₄₉N₃O₂: 1530.3933, found: 1530.4110 (M⁺). MP: > 300 °C.

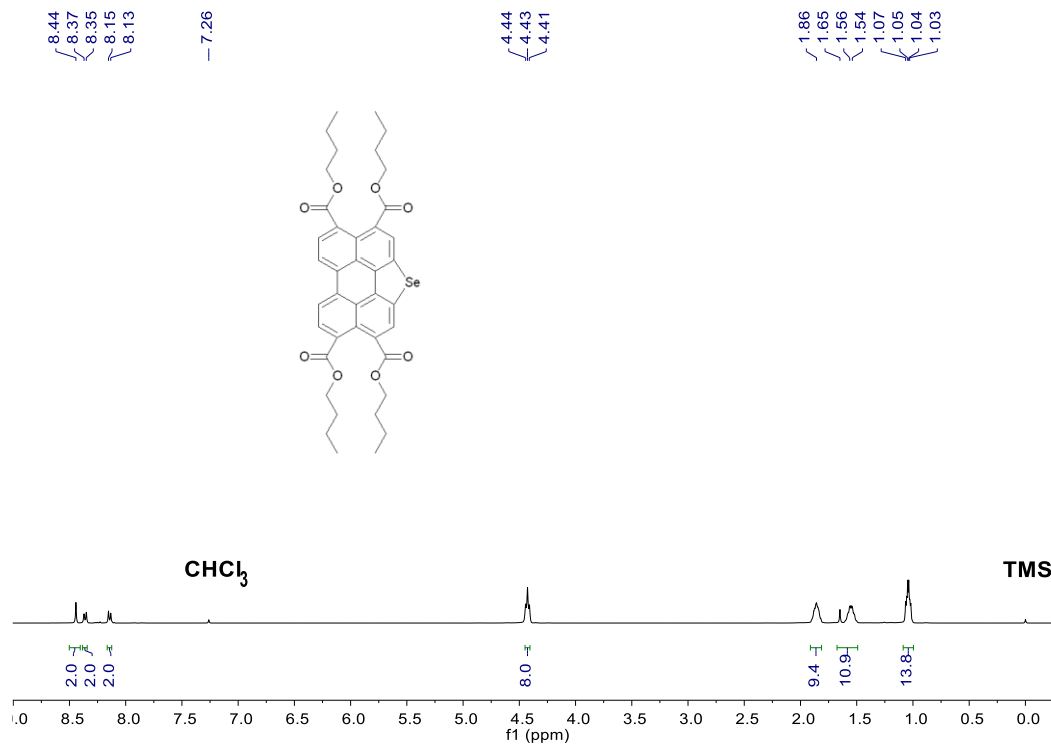
Synthesis of TBPDA-Se. 6 (0.50 g, 0.33 mmol) was dropwisely added to 15 mL ClSO₃H at 0 °C. After stirring at room temperature for 4 h, the mixture was poured into the ice, filtered, washed with water and ethanol. TBPDA-Se (0.33 g, 100%) was obtained as a red solid. It was used directly in the next step without further purification because of poor solubility. MP: > 300 °C.

Synthesis of TBPDI-Se-C₁₁. A mixture of TBPDA-Se (0.50 g, 0.50 mmol), 1-pentylhexylamine (0.51 g, 2.97 mmol), and imidazole (50 g) was stirred at 150 °C for 4 h under argon. The mixture was extracted with CHCl₃, washed with water, and purified through silica gel column chromatography. The eluent is petroleum ether/CH₂Cl₂ (1:1, v/v). TBPDI-Se-C₁₁ (0.33 g, 41%) was obtained as the orange solid. ¹H NMR (400 MHz, CDCl₃) δ 10.61 (d, 2H), 10.29 (s, 2H), 9.85 (d, 6H), 5.50 (s, 3H), 5.04 (s, 1H), 2.26–0.88 (m, 92H). ¹³C NMR (100 MHz, CDCl₃) δ 141.31, 134.25, 130.76, 129.10, 127.68, 127.28, 124.93, 124.49, 124.15, 123.82, 122.61, 122.09, 77.30, 76.98, 76.66, 55.34, 32.59, 31.88, 31.39, 29.59, 26.81, 23.78, 22.58, 19.63, 14.07, 13.53 ppm. HRMS (MALDI-TOF): Calcd for C₃₂H₄₉N₃O₂: 1622.6028, found: 1622.6022 (M⁺). MP: > 300 °C.

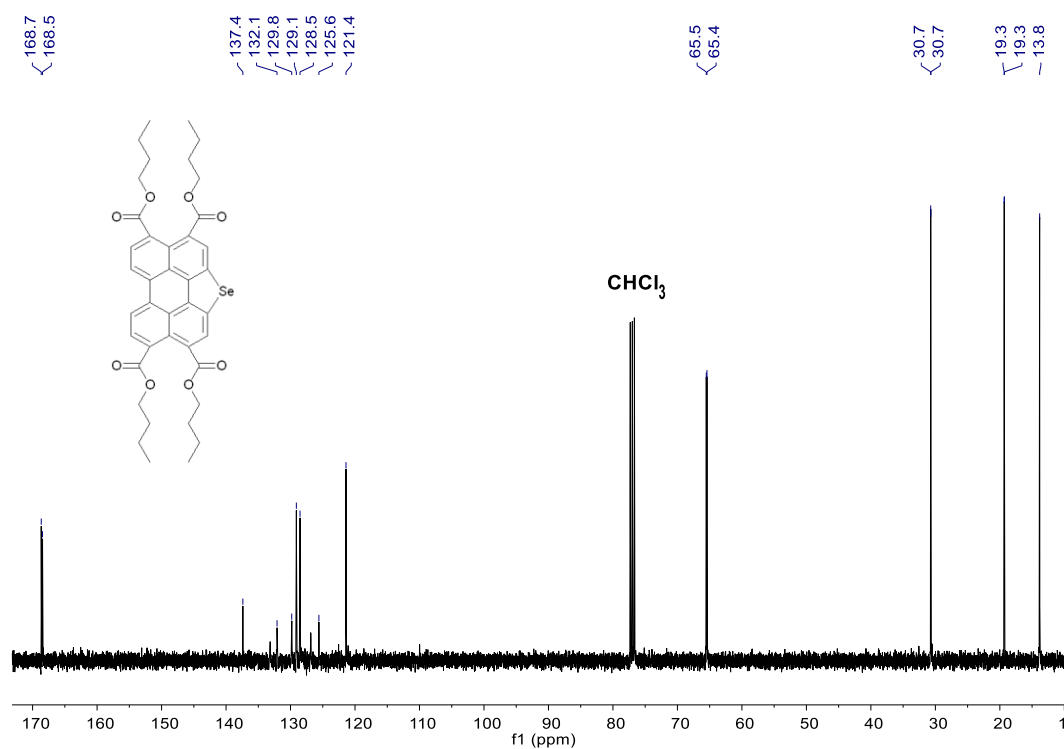
Synthesis of TBPDI-Se-C₂₃. A mixture of TBPDI-Se (0.50 g, 0.50 mmol), 1-undecyldodecyl amine (1.01 g, 2.97 mmol), and imidazole (50 g) was stirred at 150 °C for 4 h under argon. The mixture was extracted with CHCl₃, washed with water, and purified through silica gel column chromatography. The eluent is petroleum ether/CH₂Cl₂ (1:1, v/v). TBPDI-Se-C₂₃ (0.47 mg, 41%) was obtained as the orange solid. ¹H NMR (400 MHz, CDCl₃) δ 10.56 (s, 2H), 10.34 (s, 2H), 9.87 (s, 6H), 5.47 (m, 4H), 2.38–0.88 ppm (m, 188H). ¹³C NMR (100 MHz, CDCl₃) δ 165.5, 164.5, 141.4, 133.9, 130.7, 128.9, 127.4, 125.0, 124.4, 124.2, 123.5, 122.5, 121.9, 42.8, 31.9, 29.6, 27.1, 23.3, 14.1 ppm. HRMS (MALDI-TOF): Calcd for C₃₂H₄₉N₃O₂: 2295.3540, found: 2295.3580 (M⁺). MP: > 300 °C.

S3. NMR spectra

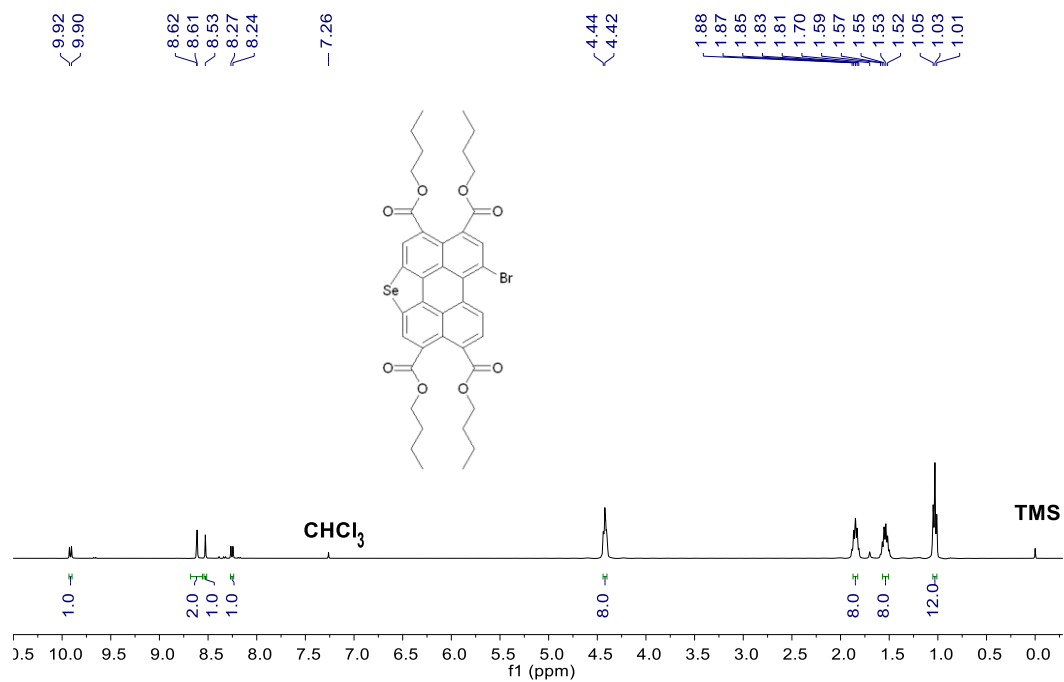
S3.1. ^1H NMR of **3** in CDCl_3 (400 MHz)



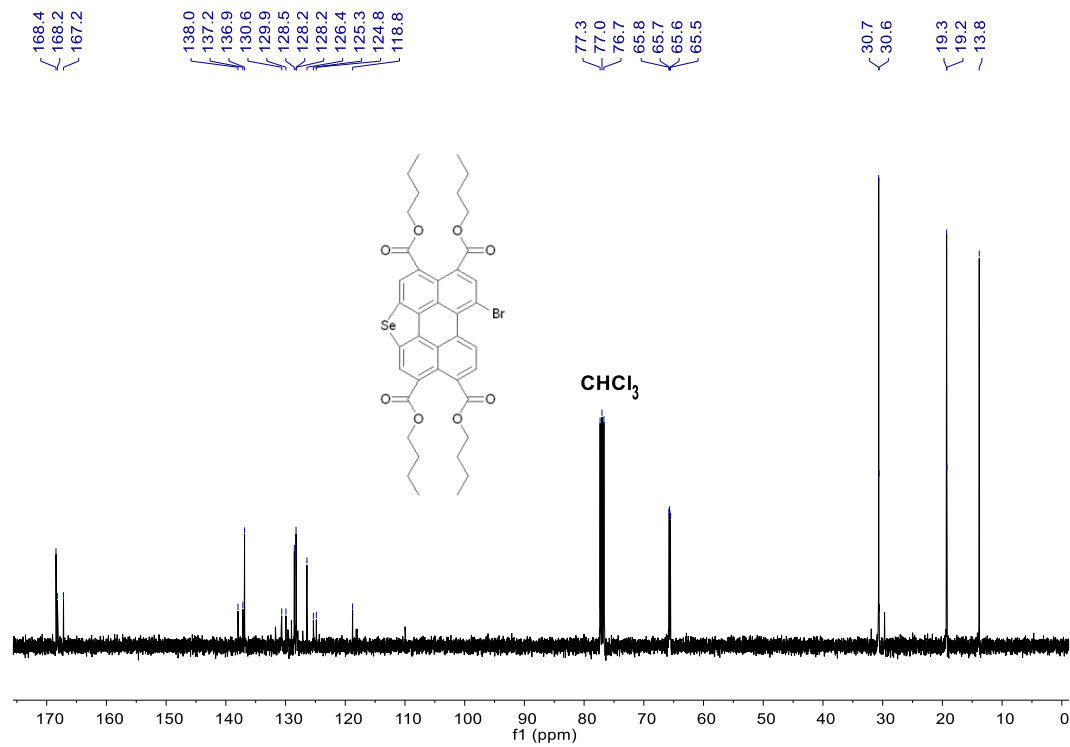
S3.2. ^{13}C NMR of **3** in CDCl_3 (100 MHz)



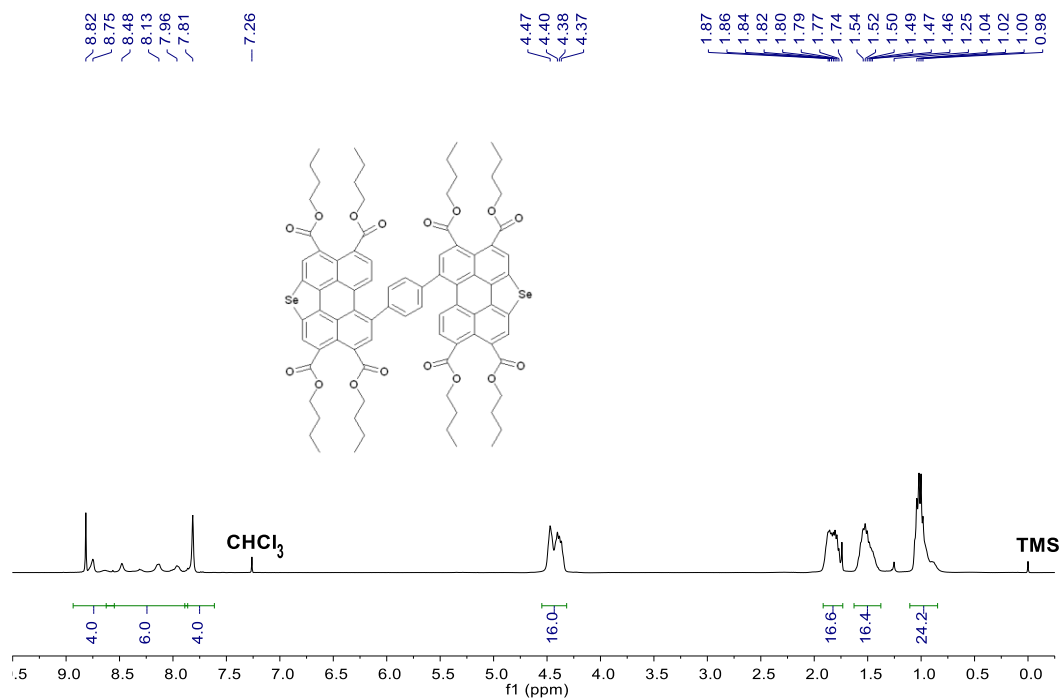
S3.3. ^1H NMR of **4** in CDCl_3 (400 MHz)



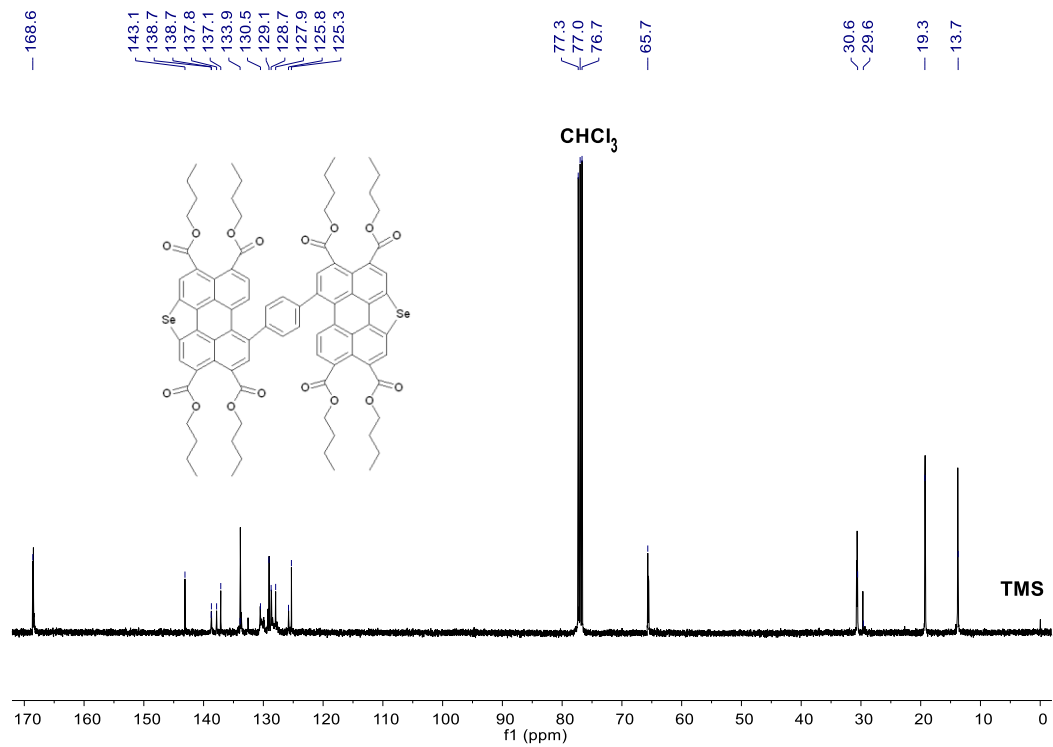
S3.4. ^{13}C NMR of **4** in CDCl_3 (100 MHz)



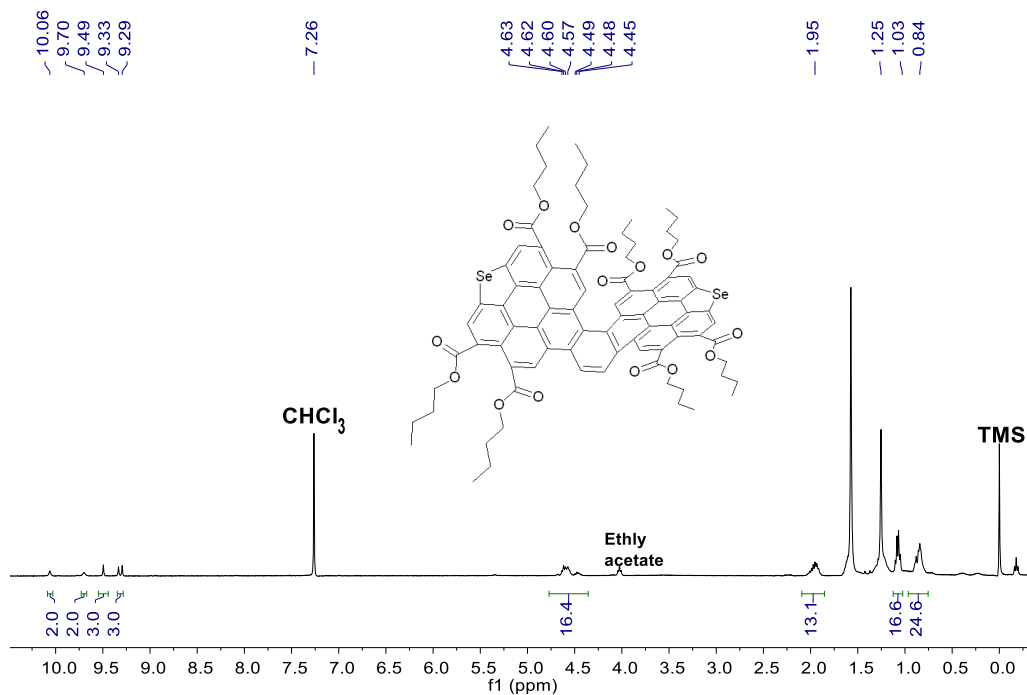
S3.5. ^1H NMR of **5** in CDCl_3 (400 MHz)



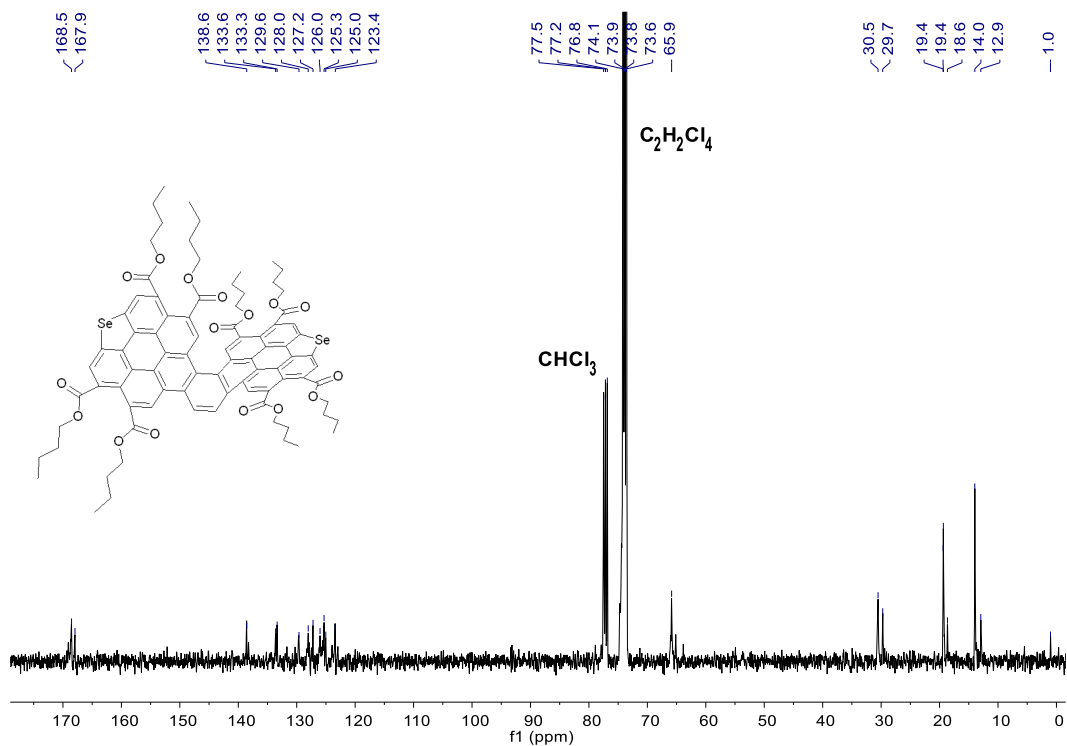
S3.6. ^{13}C NMR of **5** in CDCl_3 (100 MHz)



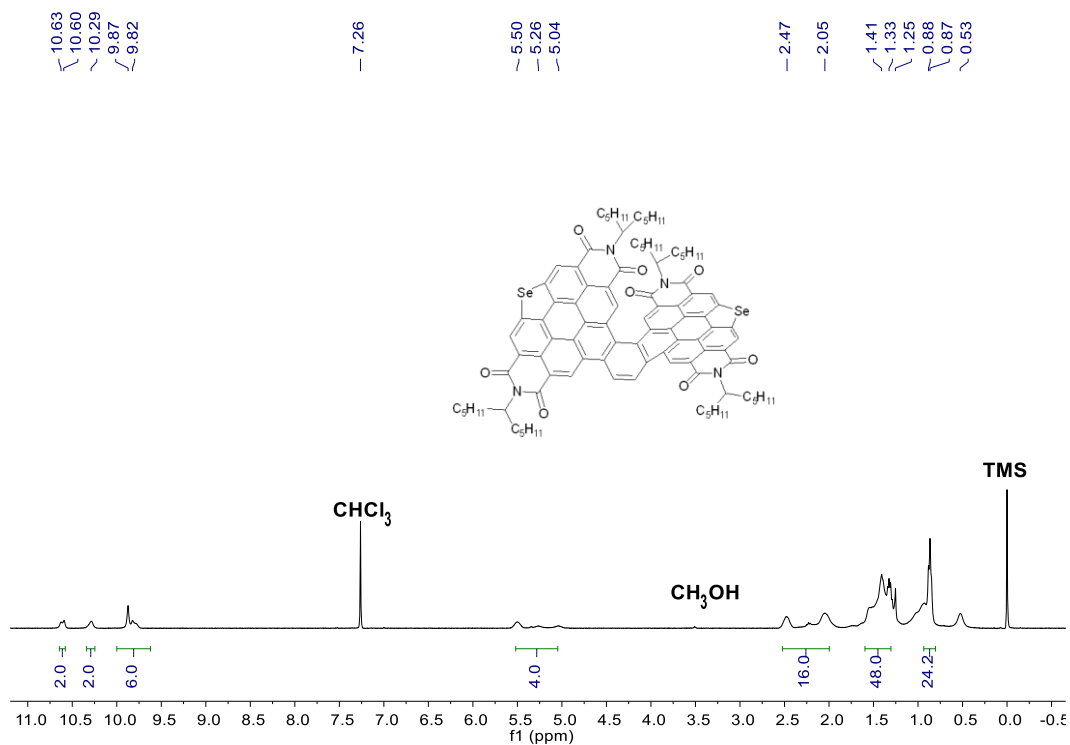
S3.7. ^1H NMR of **6** in CDCl_3 (400 MHz)



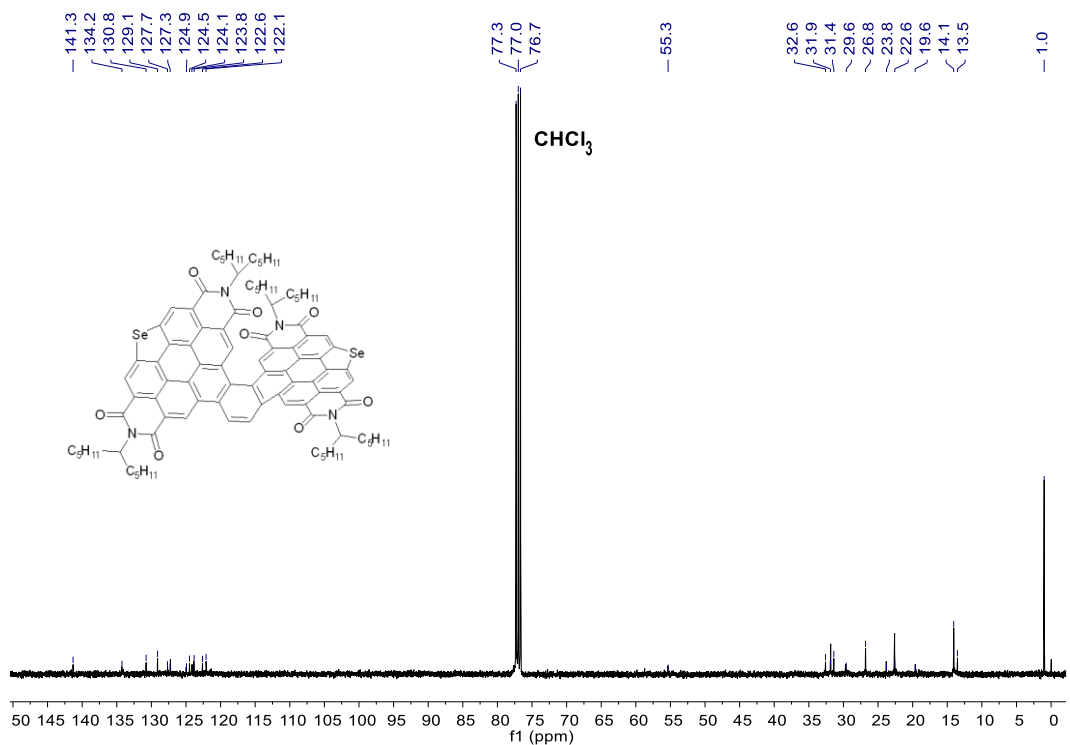
S3.8. ^{13}C NMR of **6** in CDCl_3 (400 MHz)



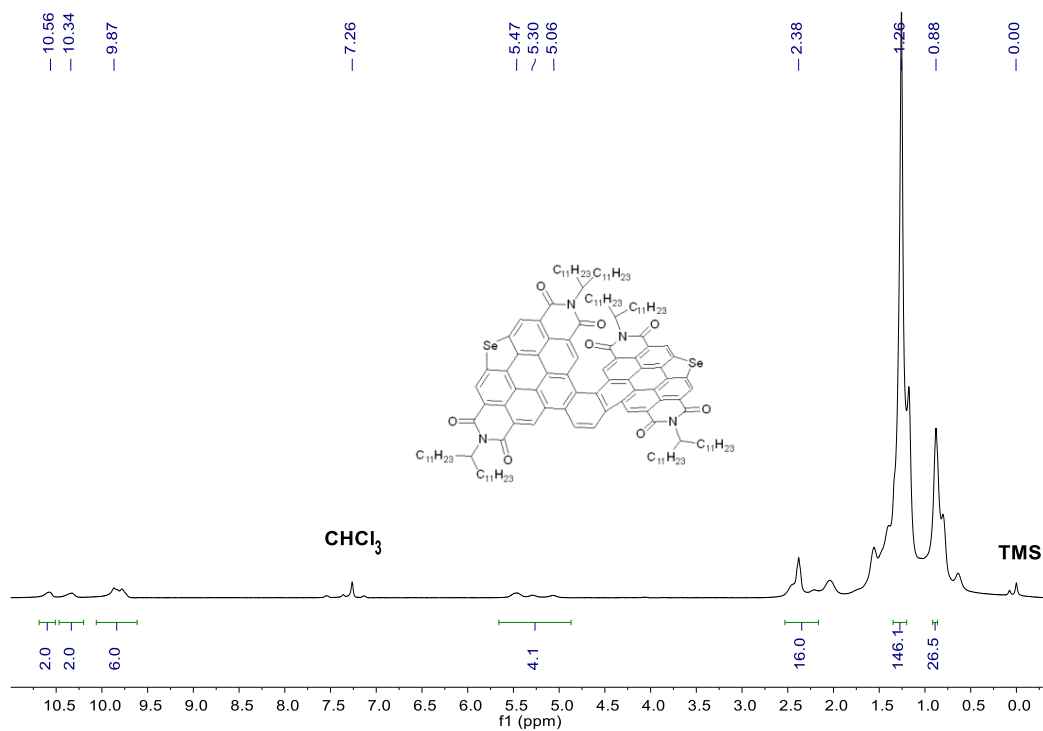
S3.9. ^1H NMR of **TBDPDI-Se-C₁₁** in CDCl_3 (400 MHz)



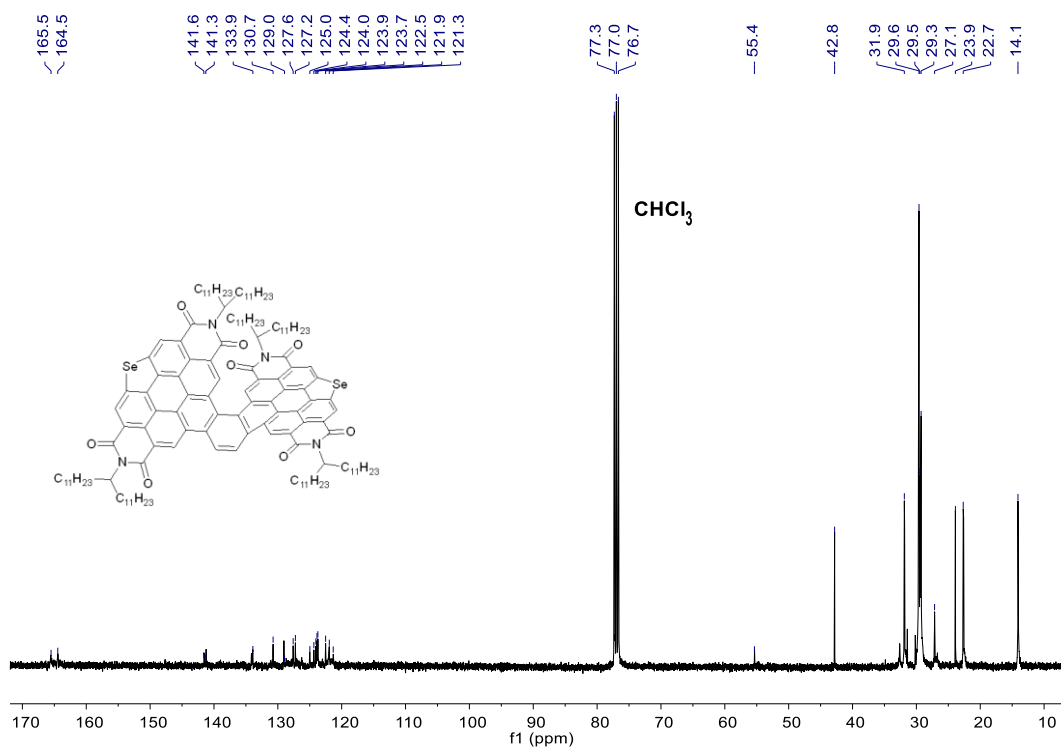
S3.10. ^{13}C NMR of **TBDPDI-Se-C₁₁** in CDCl_3 (100 MHz)



S3.11. ^1H NMR of TBDPDI-Se-C₂₃ in CDCl₃ (400 MHz)



S3.12. ^{13}C NMR of TBDPDI-Se-C₂₃ in CDCl₃ (100 MHz)



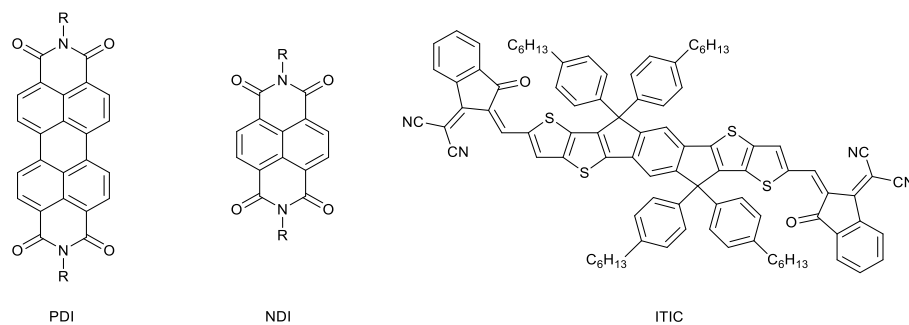


Fig. S1. Structure of PDI, NDI and ITIC

S4. TGA curves of TBDPDI-Se-C₁₁ and TBDPDI-Se-C₂₃.

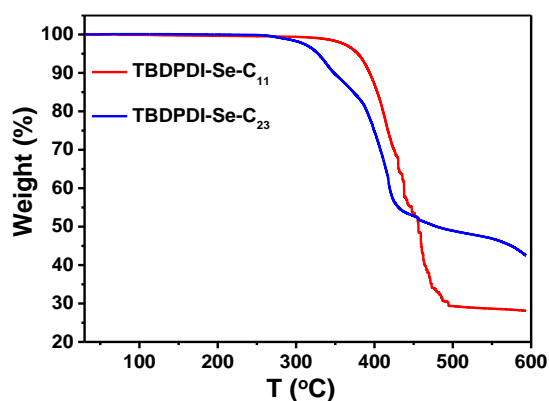


Fig. S2. TGA of TBDPDI-Se-C₁₁ and TBDPDI-Se-C₂₃

S5. DSC curves of TBDPDI-Se-C₁₁ and TBDPDI-Se-C₂₃.

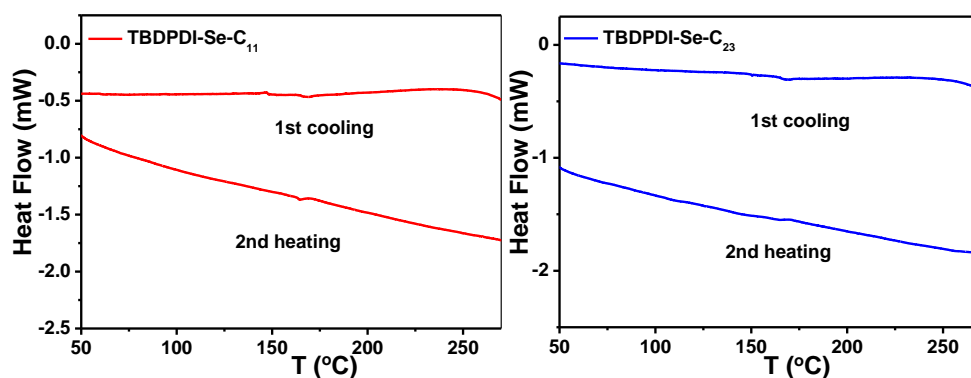


Fig. S3. DSC of TBDPDI-Se-C₁₁ and TBDPDI-Se-C₂₃

S6. UV-visible absorption.

The UV-vis absorption was recorded on a Perkin Elmer Lambda 750 spectrophotometer. The solution absorption was measured in 10^{-5} mol L⁻¹ in chloroform. The molar extinction coefficient (ϵ) was obtained from the Beer-Lambert's equation:

$$I = I_0 \times 10^{-\epsilon cl}$$

where, I and I_0 are the incident and transmitted light intensity, respectively, l is the path length, and c is the analyte concentration. To measure thin film absorption, acceptor solution ($15 \text{ mg}\cdot\text{mL}^{-1}$) in chlorobenzene was spin-coated onto quartz substrates at 800 rpm for 1 min.

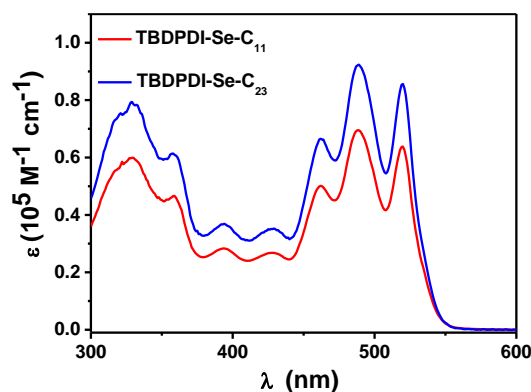


Fig. S4. UV-visible absorption spectra of TBDPDI-Se-C₁₁ and TBDPDI-Se-C₂₃ in solution

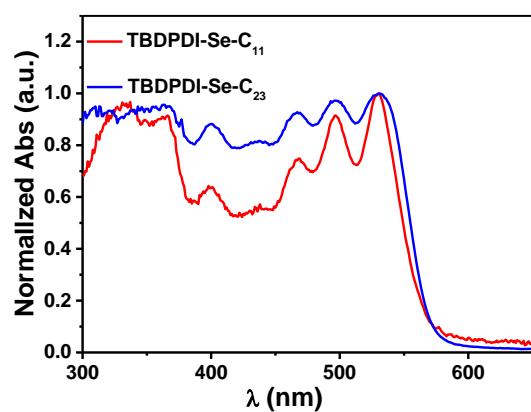


Fig. S5. Normalized UV-visible absorption spectra of TBDPDI-Se-C₁₁ and TBDPDI-Se-C₂₃ in film

S7. DFT calculations

Density functional theory (DFT) calculation was performed with basic set of B3LYP/6-311G (d, p). The long-branched alkyl chain was replaced by methyl to simplify the calculation, because they have little effect on the electron density of conjugated cores. The calculated LUMO energy levels, HOMO energy levels, and the electronic cloud distribution are as following.

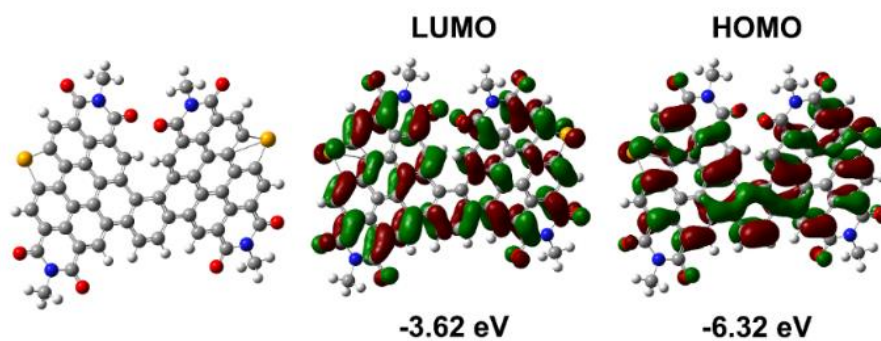


Fig. S6. Simulated molecular geometries and energy levels of TBDPDI-Se

S8. Cyclic voltammetry.

Cyclic voltammetry measurements were performed by using an electrochemical work station with a three-electrode system, with a Ag/Ag⁺ reference electrode in saturated KCl, a platinum mesh counter electrode, and a platinum wire working electrode. Organic semiconductors were drop-cast onto the electrode from CHCl₃ solution to form thin films. 0.1 mol L⁻¹ Bu₄N⁺PF₆⁻ in acetonitrile was used as the supporting electrolyte. A ferrocene/ferrocenium (Fc/Fc⁺) was used as the internal standard. LUMO energy levels were calculated based on the assumption that the energy level of Fc/Fc⁺ is -4.8 eV vs vacuum.

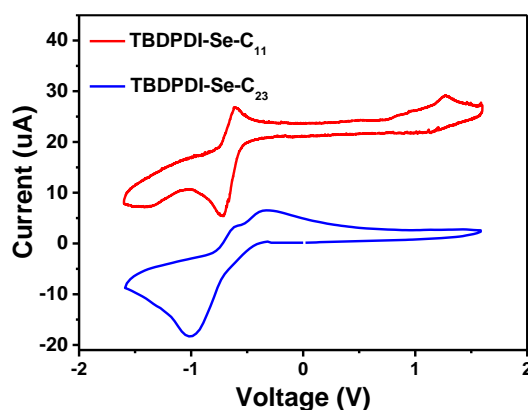


Fig. S7. CV of TBPDI-Se-C₁₁ and TBPDI-Se-C₂₃

S9. Optimization of the fabricating conditions of solar cells

Organic photovoltaic (OPV) devices were fabricated with an inverted structure of ITO/ZnO/active layer/MoO₃/Ag. The conductive ITO substrates were sequentially cleaned with ultrasonication in detergent, water, acetone, and isopropanol. After drying the ITO substrates and treating the surface with UV ozone for 20 min. The ZnO precursor solution was prepared by dissolving 0.5 g of zinc acetate dihydrate (Zn (CH₃COO)₂·2H₂O, 99.9%) in 5 mL 2-methoxyethanol (CH₃OCH₂CH₂OH, 99.8%) and 138 μ L ethanolamine (NH₂CH₂CH₂OH, 99.8%). The ZnO precursor solution was spun-coated at 4000 r.p.m. for 1 min onto the ITO surface. After being baked at 200 °C for 60 min in air, the substrates were transferred into a nitrogen-filled glove box. The optimized solution of active layers (1.5:1 weight ratio, 15 mg/mL in total weight concentration) in chlorobenzene were spun-coated at 1500 rpm resulting in the optimized active layers thickness is about 100 nm determined by AFM. MoO₃ (7 nm) and Ag (90 nm) were deposited by thermal evaporation under a vacuum chamber to complete the device fabrication. The effective area of one cell was 0.04 cm². The current-voltage (*J-V*) characteristics were measured by a Keithley 2400 Source Meter under simulated solar light (100 mW cm², AM 1.5 G, Abet Solar Simulator Sun 2000). The incident photon-to-electron conversion efficiency (IPCE) spectra were detected on an IPCE measuring system (Oriel Cornerstone monochromator equipped with Oriel 70613NS QTH lamp). All the measurement was performed at room temperature under nitrogen atmosphere.

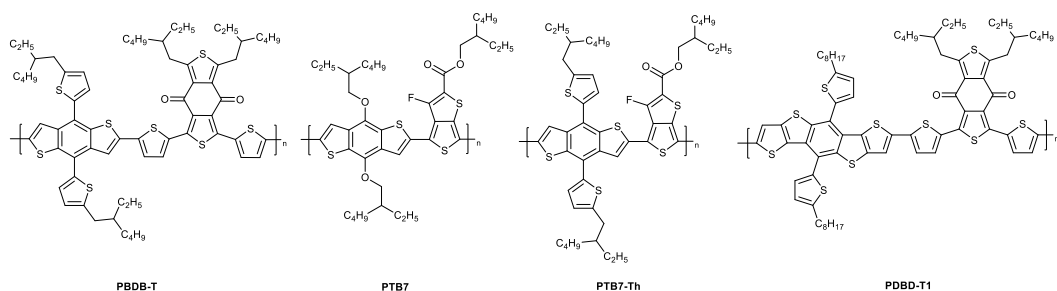


Fig. S8. Structures of PBDB-T, PTB7, PTB7-Th, and PDBD-T1.

Table S1. Photovoltaic properties of the OSCs based on TBDPDI-Se-C₁₁ with different donor (D: A = 6 mg/mL: 6 mg/mL).

Materials	V_{oc} [V]	J_{sc} [mA cm ⁻²]	FF [%]	PCE [%]
PBDB-T: TBDPDI-Se-C ₁₁	1.00	9.40	57.00	5.34
PTB7: TBDPDI-Se-C ₁₁	0.90	9.39	40.01	3.37
PTB7-Th: TBDPDI-Se-C ₁₁	0.92	9.41	38.72	3.36
PDBT-T1: TBDPDI-Se-C ₁₁	0.81	9.16	48.57	3.60

All devices were measured under the illumination of AM 1.5G, 100 mW cm⁻²

Table S2. Photovoltaic properties of the OSCs based on TBDPDI-Se-C₁₁ with different D/A ratios.

D/A [w/w]	V_{oc} [V]	J_{sc} [mA cm ⁻²]	FF [%]	PCE [%]
15:10	0.99	10.29	50.75	5.15
12:6	1.00	11.67	54.16	6.30
9:6	1.01	10.91	58.09	6.37
6:6	1.00	9.40	57.00	5.34
6:4	0.98	9.28	53.83	4.91

All devices were measured under the illumination of AM 1.5G, 100 mW cm⁻²

Table S3. Photovoltaic properties of the OSCs based on PBDB-T:TBDPDI-Se-C₁₁ (D: A=9:6) with different additives treatment.

Additives	V_{oc} [V]	J_{sc} [mA cm ⁻²]	FF [%]	PCE [%]
w/o	1.01	10.91	58.09	6.37
1%CN	1.00	7.99	53.96	4.30
1%DIO	0.98	4.55	58.81	2.61
1%NMP ^a	/	/	/	/
1%DPE	1.00	9.74	58.88	5.72

^a The PCE can not be measured by 1% NMP treatment.

All devices were measured under the illumination of AM 1.5G, 100 mW cm⁻²

Table S4. Photovoltaic properties of the OSCs based on PBDB-T: TBDPDI-Se-C₁₁ (D:A=9: 6) with different thermal annealing temperature.

TA	V_{oc}	J_{sc}	FF	PCE
[°C]	[V]	[mA cm ⁻²]	[%]	[%]
w/o	1.01	10.91	58.09	6.37
100	1.01	11.34	64.41	7.41
150	0.99	11.70	59.93	6.95
180	0.98	11.08	57.85	6.29

All devices were measured under the illumination of AM 1.5G, 100 mW cm⁻²

S10. *J-V* Curves for carrier mobility

Hole and electron mobilities were measured using the space charge limited current (SCLC) method, with hole-only device of ITO/poly(3,4-ethylenedioxythiophene): polystyrene sulfonate (PEDOT:PSS)/ active layer/MoO₃/Ag and electron-only device ITO/ZnO/active layer/Ca/Al by taking current-voltage curve in the range of -5.0 V~5.0 V. The SCLC mobilities were calculated by MOTT-Gurney equation, which is described by:

$$J = 9\varepsilon_0\varepsilon_r\mu V^2/8L^3$$

Where J is the current density, L is the film thickness of active layer, ε_0 is the permittivity of free space (8.85×10^{-12} F m⁻¹), ε_r is the relative dielectric constant of transport medium, μ is the internal voltage in the device. $V = V_{app} - V_r - V_{br}$, where V_{app} is the applied voltage to the device, V_r is the voltage drop due to contact resistance and series resistance across the electrodes, and V_{br} is the built-in voltage due to the relative work function difference of the two electrodes.²

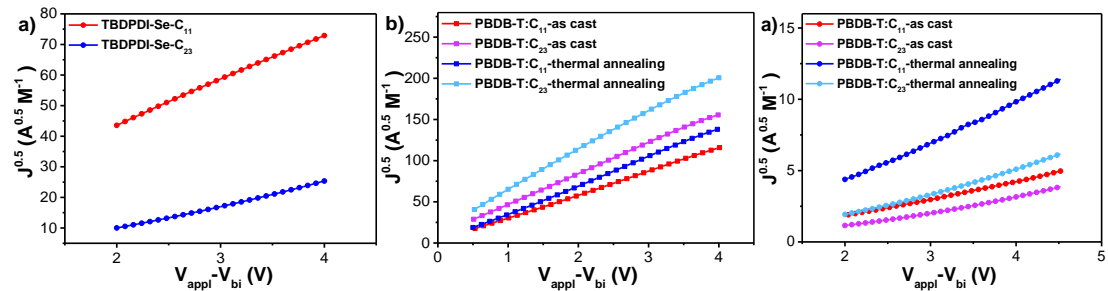


Fig. S9. (a) Current density–voltage and SCLC fitting curves of TBDPDI-Se-C₁₁ and TBDPDI-Se-C₂₃ electron only devices, PBDB-T:TBDPDI-Se-C₁₁ and PBDB-T:TBDPDI-Se-C₂₃ blend films (b) hole only devices and (c) electron only devices.

Table S5. Electron and hole mobility of acceptor films and blend films.

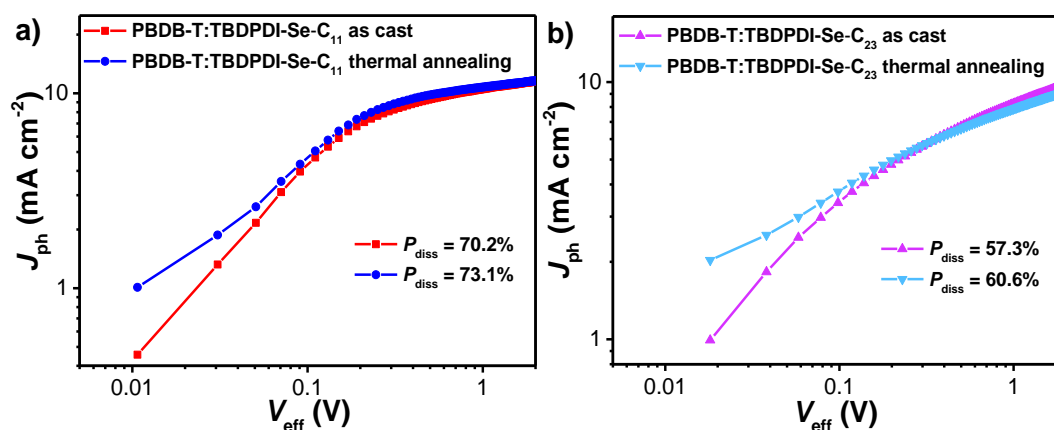
Materials	μ_{h} $\text{cm}^2 \text{V}^{-1} \text{s}^{-1}$	μ_{e} $\text{cm}^2 \text{V}^{-1} \text{s}^{-1}$	$\mu_{\text{h}}/\mu_{\text{e}}$ $\text{cm}^2 \text{V}^{-1} \text{s}^{-1}$
TBDPDI-Se-C ₁₁	/	4.72×10^{-4}	/
PBDB-T:TBDPDI-Se-C ₁₁	2.73×10^{-4}	5.24×10^{-6}	52.10
PBDB-T:TBDPDI-Se-C ₁₁ ^a	3.89×10^{-4}	2.60×10^{-5}	11.12
TBDPDI-Se-C ₂₃	/	1.36×10^{-4}	/
PBDB-T:TBDPDI-Se-C ₂₃	4.67×10^{-4}	4.87×10^{-7}	958.93
PBDB-T:TBDPDI-Se-C ₂₃ ^a	8.05×10^{-4}	1.09×10^{-6}	738.53

^aThermal annealing at 100 °C for 10 min.

S11. Charge separation and recombination dynamics

To investigate the charge generation and dissociation process of these materials, the photo-generated current density ($J_{\text{ph}} = J_{\text{L}} - J_{\text{D}}$, J_{L} : current density under illumination; J_{D} : current density in the dark) versus the effective voltage ($V_{\text{eff}} = V_0 - V_{\text{a}}$, V_0 : the voltage when the J_{ph} is zero; V_{a} : applied voltage) of the BHJOSCs were measured (Fig. 4a and 4b).³ At high V_{eff} (> 2 V), all the photogenerated excitons were dissociated into free charge carriers and collected by electrodes, and the saturation photocurrent density (J_{sat}) was only limited by the absorbed incident photons. Therefore, the P_{diss} , which is determined by normalizing J_{sc} with J_{sat} ($P_{\text{diss}} = J_{\text{sc}}/J_{\text{sat}}$) was also calculated to evaluate the exciton dissociation and charge recombination.⁴

The photocurrent (J_{ph}) and V_{oc} versus light intensity (P_{light}) were used to quantify the charge recombination dynamics. The correlation between J_{sc} and P_{light} could be expressed as a power-law equation of $J_{\text{sc}} \propto P_{\text{light}}^{\alpha}$.⁵ If all free charge carriers are swept out and collected at the electrodes prior to recombination, α is supposed to be 1, while $\alpha < 1$, bimolecular recombination somewhat exists. The slopes of V_{oc} versus $\log(P_{\text{light}})$ helps us to determine the degree of trap-assisted recombination in the devices. A slope at kT/q implies that bimolecular recombination is the dominating mechanism, where k is Boltzmann's constant, T is temperature and q is elementary charge⁶



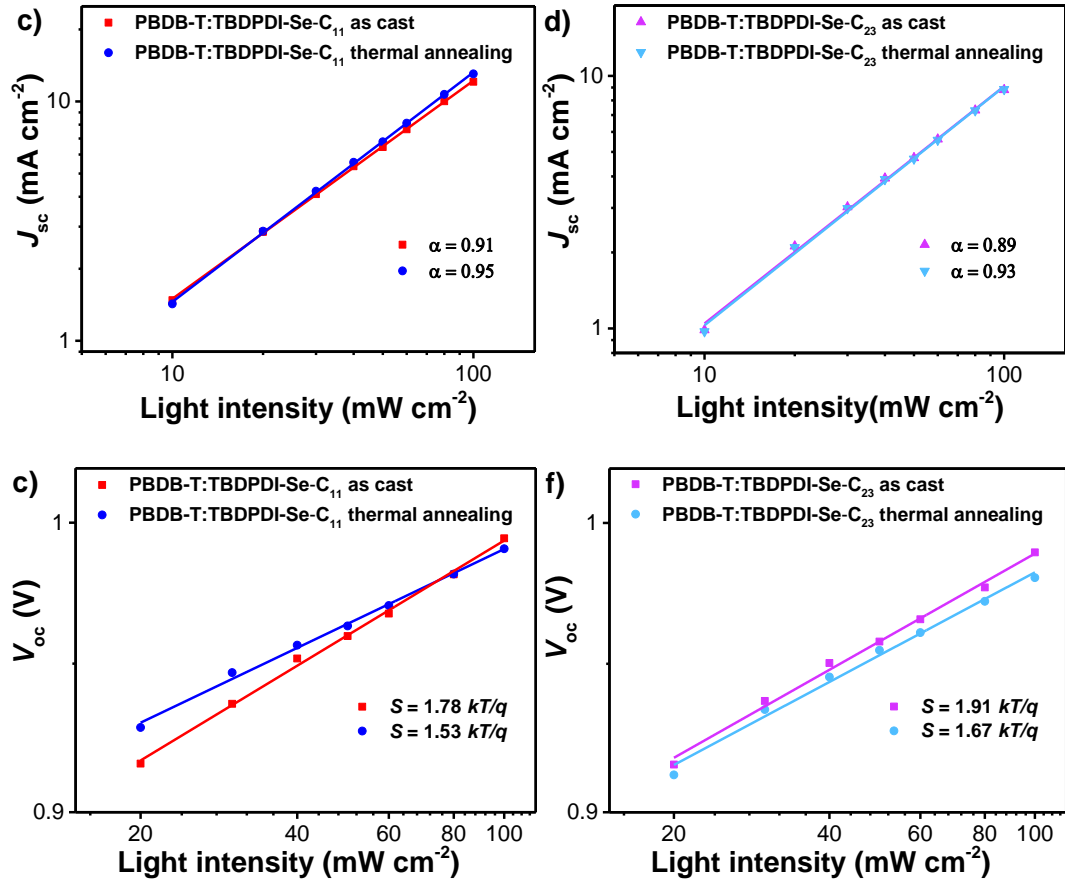


Fig. S10. (a, b) J_{ph} versus V_{eff} characteristics, (c, d) J_{sc} versus light intensity, and (e, f) V_{oc} versus light intensity of TBDPDI-Se-C₁₁- and TBDPDI-Se-C₂₃-based solar cells with/without thermal annealing.

S12. AFM images of the blend films

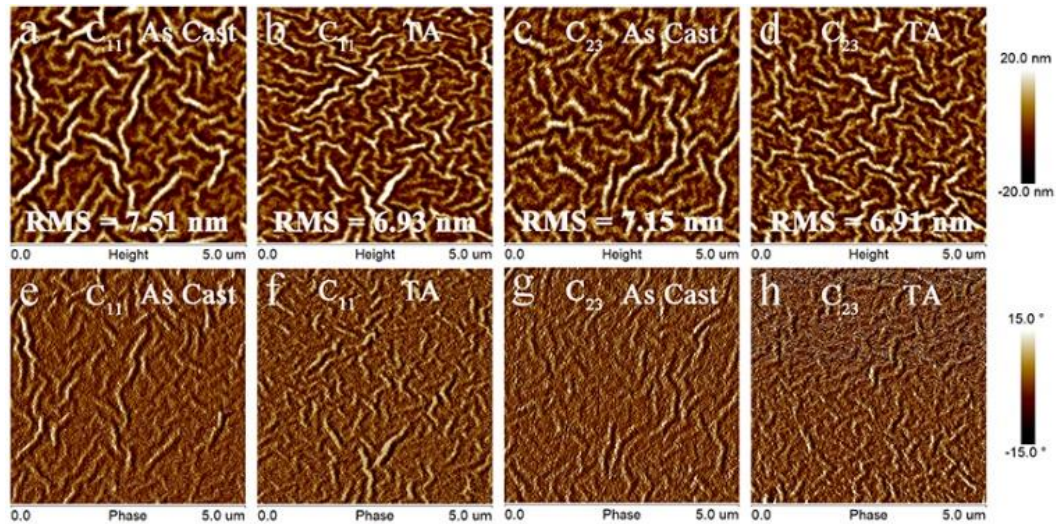


Fig. S11. (a-d) AFM height, and (e-h) phase images (scale bar: 5 μm) of blend films; PBDB-T:TBDPDI-Se-C₁₁ (a, e) without and (b, f) with thermal annealing, PBDB-T:TBDPDI-Se-C₂₃ (c, g) without and (d, h) with thermal annealing.

S13. TEM images of the blend films

Transmission electron microscopy (TEM) images were taken on a JEOL-2100F transmission electron microscope and an internal charge-coupled device (CCD) camera. The specimens for TEM measurement were prepared by spin casting the blend solution on ITO/PEDOT:PSS substrates, the films were floated on a water surface, and transferred to TEM grids.

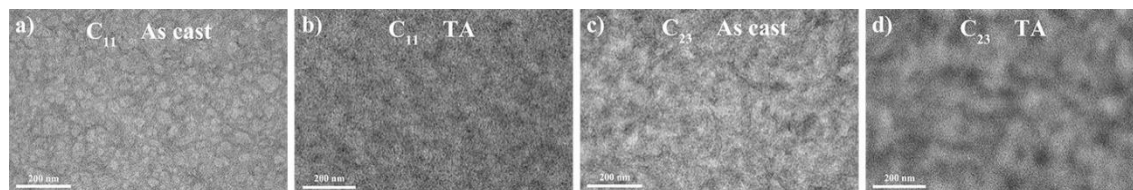


Fig. S12. TEM images (scale bar: 200 nm) of blend films; PBDB-T:TBDPDI-Se-C₁₁ (a) without and (b) with thermal annealing, PBDB-T:TBDPDI-Se-C₂₃ (c) without and (d) with thermal annealing.

Reference

- 1 S. Li, L. Ye, W. Zhao, S. Zhang, S. Mukherjee, H. Ade and J. Hou, *Adv Mater*, 2016, **28**, 9423-9429.
- 2 (a) A. Babel and S. A. Jenekhe, *J. Am. Chem. Soc.*, 2003, **125**, 13656-13657; (b) M. M. Alam and S. A. Jenekhe, *Chem. Mater.*, 2004, **16**, 4647-4656; (c) U. Scherf, *J. Mater. Chem.*, 1999, **9**, 1853-1864.
- 3 Q. Wu, D. Zhao, A. M. Schneider, W. Chen and L. Yu, *J. Am. Chem. Soc.*, 2016, **138**, 7248-7251.
- 4 P. Schilinsky, C. Waldauf and C. J. Brabec, *Appl. Phys. Lett.*, 2002, **81**, 3885-3887.
- 5 V. D. Mihailechi, H. X. Xie, B. de Boer, L. J. A. Koster and P. W. M. Blom, *Adv. Funct. Mater.*, 2006, **16**, 699-708.
- 6 (a) S. R. Cowan, A. Roy and A. J. Heeger, *Physical Review B*, 2010, **82**, 245207; (b) L. Lu, W. Chen, T. Xu and L. Yu, *Nat. Commun.*, 2015, **6**, 7327.